Ceramics-Silikáty 65 (2), 148-157 (2021)
www.ceramics-silikaty.cz doi: 10.13168/cs.2021.0014

EFFECTS OF COAL GANGUE ON THE SULFATE ATTACK RESISTANCE OF CEMENT-BASED MATERIALS

GUANGLIN DING*, **, #JUN YANG***, ZHIJUN YANG*, **

*Evergrande Real Estate Group, Chengdu, Sichuan, China, 610094
**Evergrande Travel Group Sichuan Company, Chengdu, Sichuan, China, 610094
***Xindu Industrial Park Management Committee, Chengdu, Sichuan, China, 610500

#E-mail: yangjunwell@163.com

Submitted December 9, 2020; accepted February 19, 2021

Keywords: Coal gangue, Cement-based materials, Sulfate attack resistivity

Coal gangue contains a certain amount of active ingredients; it can be used as an addition to cement-based materials after activation. However, the durability of cement-based materials with a calcined coal gangue addition should be studied. In this paper, the sulfate attack resistivity of cement-based materials with a calcined coal gangue addition was studied and compared with ordinarily used fly ash. The effects of the sulfate attack resistance on the strength development, volume change and microstructure of the cement paste, mortar and concrete were studied. It was found that calcined coal gangue effectively improved the sulfate attack resistivity of cement-based materials, specifically expressed by the reduction in the strength loss or volume expansion of the mortar or concrete under the sulfate attack. When compared with the fly ash added samples, coal gangue exhibited a better improvement in the sulfate attack resistivity through the analysis of the strength loss and expansion results.

INTRODUCTION

Sulfate attack resistivity of cement-based materials is a serious concern of structures serving in a marine environment, in seawater, underground water, etc. [1]. In these service conditions, sulfate ions migrate into hardened cement-based materials with water, and react with calcium hydroxide and aluminate phases, and then sulfate attack products, such as ettringite or gypsum, are formed. During these processes, expansion happens due to the volume increase of the solid phases of the sulfate attack products, which usually causes cracks of cement-based materials [2-5]. Besides, the C–S–H gel could react with the sulfate ions and the gel property can become deteriorated, and the breakup of hardened cement-based materials can occur [6].

It has been well indicated that modification of the chemical composition of cementitious materials, such as the reduction of the $Ca(OH)_2$ content, modification of the C–S–H gel, as well as physical densification of the microstructure of the cementitious material, can potentially increase the sulfate attack resistivity [6-7]. Thus, the use of supplementary cementitious materials (SCMs), such as fly ash, blast furnace steel slag, and silica fume have been widely used to tackle sulfate attack. Many researches have shown that the use of SCMs increased the sulfate attack resistance of cement-based materials. The replacement part of the cement by SCMs decreased the ettringite and gypsum content, expansion ratio, strength loss and the deterioration of visual appearance under a sulfate attack [8-11]. The lower cement dosage reduced the content of the expansive products of ettringite (AFt) and gypsum under the sulfate attack resulted by the pozzolanic reaction between the CH and the SCMs, as well as the reduction of the C_3A content in the mixture due to the dilution effect [8, 11]. The reduction in the Ca/Si ratio of the C–S–H gel by the SCMs also showed a positive effect on the improvement of the sulfate attack resistance of cement-based materials [12]. However, the availability of SCMs with good quality has been limited in recent years in China [13], the durability and mechanical properties were cut down when low-quality SCMs were used in cement-based materials. Therefore, the sulfate attack resistance of cement-based materials has become a concern.

Coal gangue, an industry solid that is discharged when coal is excavated and washed in the production course of a coal mine. Coal gangue is one of the industrial solid wastes with the biggest discharge. Its output is about 15 ~ 20 % of the total coal output [14]. SiO_2 and Al_2O_3 are the main components of coal gangue. More recently, the application of coal gangue into cement-based materials has aroused great interest, and the improvement of pozzolanic reactivity and effects on the mechanical properties of cement-based materials have been studied [15-16]. The ordinary method to improve the pozzolanic reactivity of coal gangue is direct calcination, known as the thermal activation method. Some studies [15, 17-18] suggested that the generated amorphous reactive SiO_2 and Al_2O_3 from kaolinite contribute to improving the

reactivity of coal gangue after calcination. Research by Song et al [19] showed that calcined coal gangue at 700 °C has an improved activity. It was also shown in [20] that the activity of coal gangue could be enhanced by calcination between 700 °C and 900 °C. Li et al [21] indicated that the performance of coal gangue powder calcined under 700 °C was almost perfect. Liu et al. [17] calcined coal gangue for 2 h at different temperatures (500 - 900 °C) and utilised them in a cement mortar as an addition (the cement replacement level was 12 %), the results showed that a cement mortar containing calcined coal gangue calcined at 800 °C exhibited an 18 % increase in the compressive strength at 28 days. Many researchers have reported that an additional dosage of about 10 - 20 % can secure a relatively high strength. However, with a 30 % or higher replacement content, the 28-day strength of mortar was significantly decreased [22]. Yang et al. [23] studied the pore structure of a blended cement prepared with 0, 10, 20, 30 and 40 % calcined coal gangue, and found an increasing porosity with an increasing substitution level at the early age. However, the negative effect seems to be insignificant in the late age samples. Similar results have also been revealed by other studies [24-25]. If the influence of activation methods on the mechanical properties of coal gangue cement-based materials become widely investigated, long-term performance studies are also needed to evaluate the durability of these materials.

In this paper, in order to investigate the effects of coal gangue on the performance of sulfate attack resistivity, the physical and mechanical properties of coal gangue cement-based materials and fly ash cement-based materials at typical replacement levels were studied.

EXPERIMENTAL

Materials

Ordinary Portland cement (P•O 42.5), calcined coal gangue (CG) and class F fly ash (FA) were used in this study. The chemical and physical properties of the raw materials are shown in Table 1. The coal gangue showed a similar composition to the FA. The loss on ignition (LOI) was significantly reduced after calcination of the coal gangue. Moreover, 700 °C for 2 h was used for the coal gangue calcination. After being calcined, coal gangue was ground into a powder with a specific surface area of 435 $m^2 \cdot kg^{-1}$.

The SEM images of the raw materials are shown in Figure 1. Spherical particles can be seen in the fly ash, while irregular particles can be seen in the coal gangue sample. When compared with the uncalcined coal gangue, it can be found that the surface of the calcined coal gangue particles is more rough and uneven. This may be because the calcination process caused some organic components in the coal gangue to burn out and form pores.

Figure. 2 shows the XRD spectra of the coal gangue before and after calcination, it can be seen that the kaolinite was completely decomposed after calcination at 700 °C for 2 h.

Sample preparation

The mix proportions of the cement paste and mortar samples are shown in Table 2. Standard sand (GB/T 17671-1999 [26]) was used to prepare the cement mortar and a cement to sand ratio of 1:3 was used. During

Table 1. Chemical compositions of the cement, CG and FA (wt. %).

Sample	CaO	SiO_2	Al_2O_3	SO_3	Fe_2O_3	MgO	MnO	Na_2O	TiO_2	LOI
Cement	65.48	18.31	4.58	2.78	3.59	2.77	0.03	–	–	0.45
CG	6.24	42.37	26.13	0.98	16.21	1.57	0.19	1.32	3.99	9.58
Calcination CG	6.18	41.36	25.88	1.04	15.36	1.64	0.17	1.289	4.16	1.10
FA	6.28	50.47	28.33	1.43	7.62	0.70	0.04	0.93	3.76	2.11

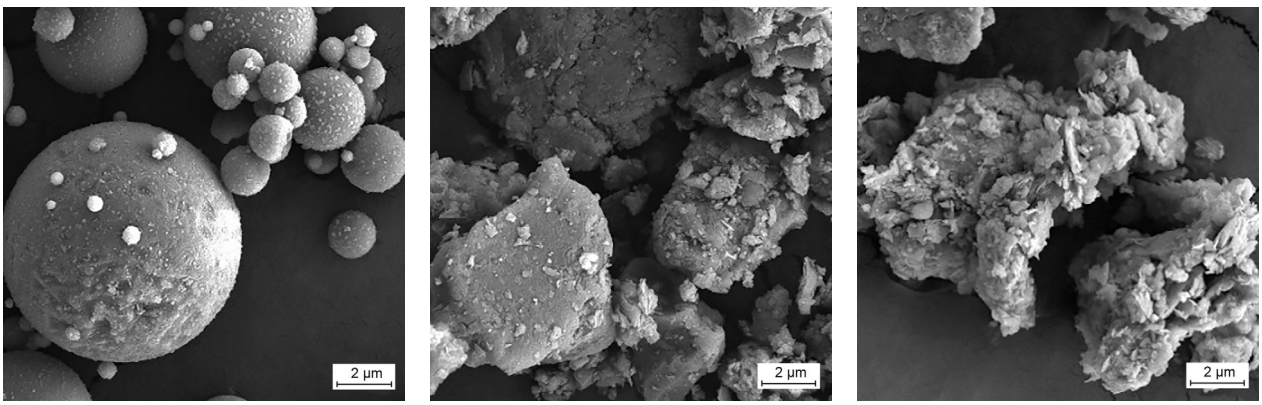

a) Fly ash b) Uncalcined coal gangue c) Calcined coal gangue

Figure 1. SEM images of the raw materials.

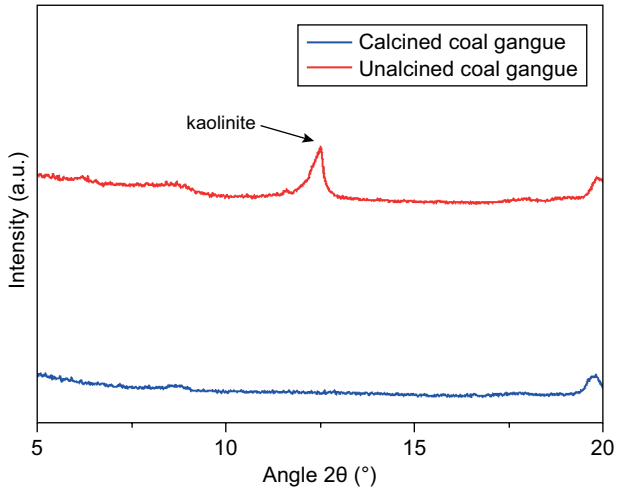

Figure 2. XRD spectra of the coal gangue before and after calcination.

mixing, the raw materials were dry-mixed for one minute and then wet-mixed for another four minutes. After mixing, the paste was cast in 4 × 4 × 4 cm moulds. The mortar was cast in 160 × 40 × 40 cm and 2.5 × 2.5 × × 28.5 cm moulds. All the samples were cured for 1 day in the ambient environment (ca. 25 °C/60 % relative humidity (RH)) before demoulding and then cured for 28 days in a chamber (20 °C/95 % RH). The cement paste samples were cut into 1 × 4 × 2 mm slices after being cured in a chamber for 28 days, and then being exposed to a sulfate solution for the XRD test. The 160 × × 40 × 40 cm cement mortar samples were exposed in a 5 wt. % Na_2SO_4 solution for 28, 180 and 360 days and the control samples were also cured with a saturated Ca $(OH)_2$ solution (C ref) for the strength test. The 2.5 × 2.5 × × 28.5 cm mortar samples were exposed in a 10 wt. % Na_2SO_4 solution for the length change test.

The mix proportions of the concrete samples are shown in Table 3. A maximum size of 2.5 cm was used for the coarse aggregate. The raw materials were dry-mixed for one minute and then wet-mixed for another four minutes. After mixing, the concrete was cast in 10 × × 10 × 10 cm moulds. The samples were cured for 1 day in the ambient environment (25 °C/60 % RH) before demoulding and then cured for 28 days in a chamber (20 °C/95 % RH). After a curing time of 28 days, the concrete samples were cured in sulfate dry-wet cycles and in a saturated $Ca(OH)_2$ solution, respectively. During the research, a 10 wt. % sodium sulfate solution was used for the sulfate attack.

Table 2. Mix proportions of the paste and mortar samples.

Samples	Paste w/b	Mortar w/b	Cement (wt. %)	CG (wt. %)	FA (wt. %)
C	0.4	0.35	100	–	–
CG10	0.4	0.35	90	10	–
CG20	0.4	0.35	80	20	–
CG30	0.4	0.35	70	30	–
FA10	0.4	0.35	90	–	10
FA20	0.4	0.35	80	–	20
FA30	0.4	0.35	70	–	30

Test method

Activity of coal gangue

The activity of the coal gangue was tested under the GB/T 1596-2017 method (Chinese standard, fly ash used for the cement and concrete [27]). The mix proportions of the samples for the activity test are shown in Table 4. The activity was calculated as follows:

$$\text{Activity} = \frac{\text{Mortar strength of CG or FA at 28 days}}{\text{Mortar strength of control at 28 days}} \times 100\ \%$$

Table 4. Mix proportions of the activity test samples.

Samples	w/b	Cement (wt. %)	CG (wt. %)	FA (wt. %)
Control	0.5	100	–	–
CG	0.5	70	30	–
FA	0.5	70	–	30

Mechanical property measurements

The flexural and compressive strength of the cement mortar samples, and the compressive strength of the mortar samples were tested by a CMT5000 Universal

Table 3. Mix proportions of the concrete samples.

Samples	Concrete w/b	Cement (wt. %)	CG (wt. %)	FA (wt. %)	Sand coarse aggregate ratio	Superplasticiser (wt. %)
C	0.4	100	–	–	0.35	0.04
CG10	0.4	90	10	–	0.35	0.04
CG20	0.4	80	20	–	0.35	0.04
CG30	0.4	70	30	–	0.35	0.04
FA10	0.4	90	–	10	0.35	0.04
FA20	0.4	80	–	20	0.35	0.04
FA30	0.4	70	–	30	0.35	0.04

Testing Machine (MTS, China) and the strength ratio was calculated to show the relationship of the sulfate attack resistance between the different samples.

$$\text{Strength ratio} = \frac{\text{Sample strength after sulfate attack or C ref}}{\text{Control sample strength after sulfate attack}} \times 100\ \%$$

$$\text{Strength change} = \frac{\text{Sample strength after sulfate attack} - \text{Sample strength cured in Ca(OH)}_2}{\text{Control sample strength after sulfate attack}} \times 100\ \%$$

For the mortar samples, the average value of three samples was used for the determination of the flexural strength values, and the average value of six measurements was used for the compressive strength values. For the concrete samples, the average value of three samples was used for the determination of the compressive strength values.

Length change

The length change of the cement mortars was calculated by ASTM C1012/C1012M – 15 [28].

$$\Delta L = (L_1 - L_2)/L_3 \times 100$$

ΔL = change in length at x age (%),
L_1 = comparator reading of the specimen at a certain age,
L_2 = initial comparator reading of the cement mortar bar comparator reading,
L_3 = nominal gauge length, 250 mm.

X-ray diffraction

The sulfate attack products of the cement paste were studied by X-ray diffraction (XRD, Bruker D8 Advance, Germany). The samples were vacuumed oven-dried at 45 °C for 72 hours and then ground into a powder smaller than 75 μm by an agate mortar after exposure in a 10 wt. % Na_2SO_4 solution for 360 days. The Cu-Kα radiation was conducted at a voltage of 40 kV and an accelerated current of 40 mA. A scan speed of 0.5 sec/step and increment of 0.02° was used.

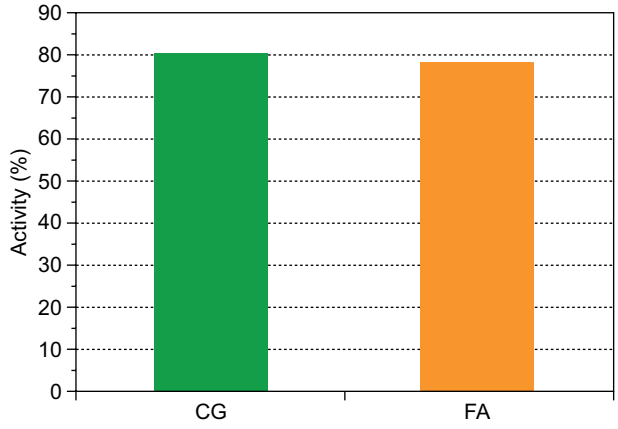

Figure 3. Activity of the fly ash and coal gangue.

Morphology and microstructure characterisation

A Scanning Electron Microscope (SEM) and Energy Dispersive Spectrometer (EDS) (JSM-7610F, JEOL, Japan) were used to identify the phase present and microstructure, respectively. The samples were vacuumed oven-dried at 50 °C for 48 hours before being tested and the fresh fracture surface of the samples was made conductive by coating a 20 nm thick platinum film onto the surface.

RESULTS AND DISCUSSIONS

Activity and strength of mortar samples

Figure 3 shows the activity of the fly ash and coal gangue, it can be seen that the activity of the coal gangue is higher than that of the fly ash. This might be related to the calcination process producing more active SiO_2 and Al_2O_3.

For the strength of the cement mortar at a curing time of 28 days (as shown in Figure 4), a lower strength was shown by the CG- and FA-added samples when compared with the control samples. With an increase in

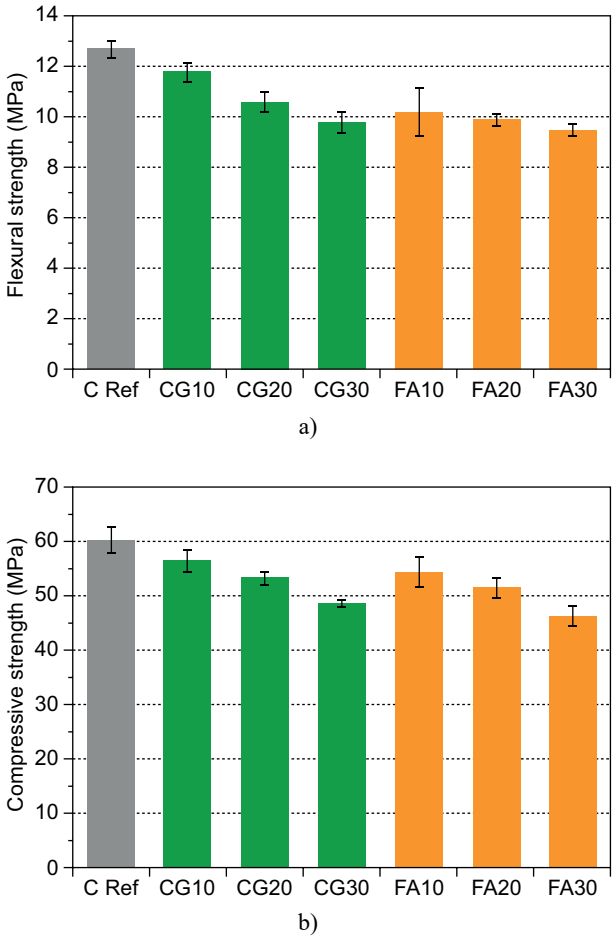

Figure 4. Flexural (a) and compressive strength (b) of the cement mortar at a curing time of 28 days.

the added dosage, the flexural strength of the CG-added samples decreased and the lowest strength of 9.8 MPa was shown by the CG30 samples. The FA-added samples have the same strength change tendency. However, at the same dosage, the FA-added samples showed a lower strength than the CG-added samples, which was consistent with the activity results in Figure 3. For the compressive strength, it decreased with an increase in the CG- and FA-added dosage. The same FA and CG dosage showed a similar strength, a slightly increased strength was shown by the CG-added samples. The high activity of the CG contributed to these results.

Flexural strength and compressive strength after sulfate attack

The flexural and compressive strength ratio of the cement mortar samples cured in the 10 wt. % Na_2SO_4 solution up to 360 days is shown in Figure 5. For the flexural strength after the sulfate attack, it can be seen that the flexural strength of the control samples was higher than the C Ref samples when cured in the Na_2SO_4 solution for 28 and 180 days. This indicated the beneficial effect of the sulfate ions on the strength development until this age, and similar results were reported by other researchers [29-30]. The main reason could be that the formation of expansive products due to the sulfate attack was not enough to damage the cement mortar at 180 days and, therefore, contributed to the densification of the microstructure.

For the 28-day sulfate attack samples, the flexural strength ratio of the CG added samples showed an increase with the added dosage, which could be due to the higher CG addition leads to the slow hydration of the mixture and the sulfate solution easily migrate inside. More sulfate attack products were formed and resulted in a higher strength ratio. The FA-added samples showed the same change with the FA added dosage increase, and a higher strength ratio was shown when compared with the same dosage added in the CG samples, which means that more sulfate attack products were formed. Moreover, the sulfate might be promoted by the reaction of the FA in the cementitious system [30-31].

When the sulfate attack time was increased to 180 days, a 15 % higher flexural strength was shown by the C samples than the C Ref samples. This result indicated that more sulfate attack products were formed, but they were not enough to damage the cement mortars. A similar flexural strength was shown by the same CG and FA added dosage samples, the strength of the FA-added sample was slightly higher than the CG-added samples, the reason was discussed before. At the sulfate attack time of 360 days, a decrease in the strength (20 % reduction when compared with the C Ref samples) of the C samples was shown. Enough sulfate attack products caused structural damage and contributed to this result. The formation of ettringite and gypsum (as shown in Figures 6 and 7) increased the volume of the solid phases and consequently the destruction of the structure occurs. The CG-added samples showed a higher strength ratio than the C samples, the substitution level of the cement and the pozzolanic reactivity of the coal gangue slag reduced the formation of sulfate attack products and, therefore, the damage process was retarded. The XRD results in Figure 6 show few sulfate attack products of ettringite and gypsum of the CG-added samples after the sulfate attack, which support the strength change results. The FA samples also showed a higher strength ratio than the C samples, the reason was similar to the CG-added samples. However, the strength ration of the FA-added

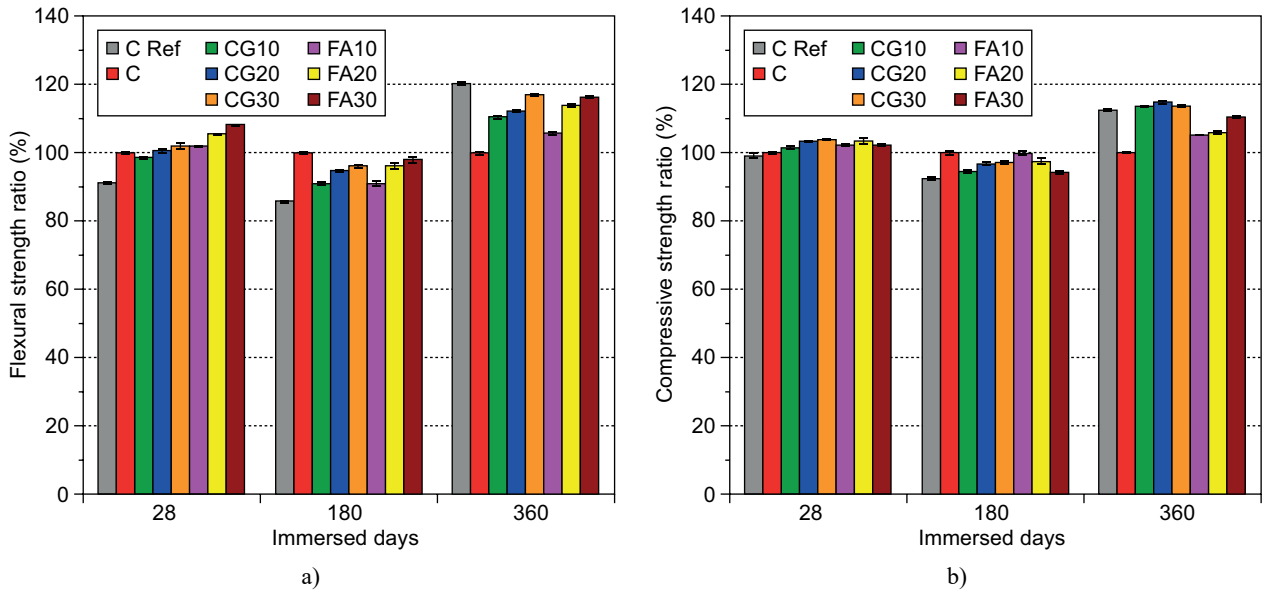

Figure 5. Flexural (a) and compressive (b) strength ratio of the cement mortar samples cured in a 10 wt. % Na_2SO_4 solution up to 360 days.

samples was lower than the CG-added samples, which indicates the better sulfate attack resistivity of the CG-added samples.

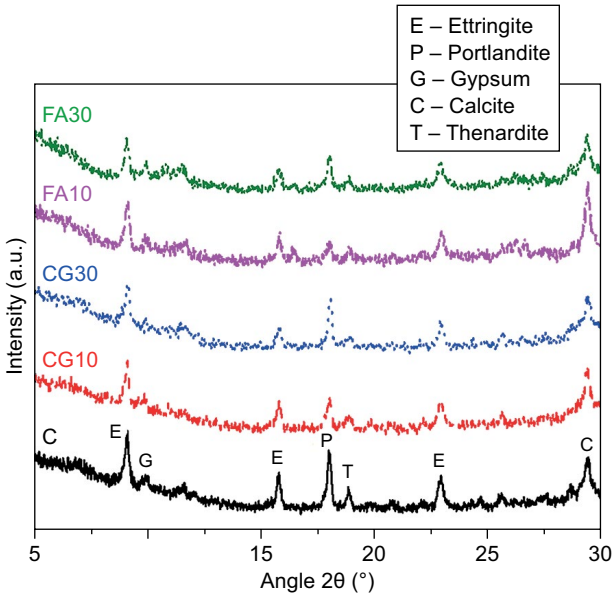

Figure 6. XRD spectra of the cement paste samples cured in a 10 wt. % Na_2SO_4 solution up to 360 days.

Figure 6 shows the XRD spectra of the cement paste after sulfate attack. It can be seen that the CG and FA addition reduced the sulfate attack content of the ettringite and gypsum. The Portlandite content is also cut down with the CG and FA addition. The CG30 and FA30 samples showed higher portlandite when compared with the CG10 and FA10 samples, and slightly less ettringite and gypsum is also shown. It means that more CH reacts with the sulfate solution in the FA10 and CG10 samples and more sulfate attack products are formed. It supports the strength change in Figure 5 and the strength loss in Figure 8.

For the compressive strength cured in 10 wt. % Na_2SO_4 solution up to 28 days, the C samples showed a slightly higher strength ratio when compared with the C Ref samples. It was different from the flexural strength ratio in Figure 5a, which could be due to the sulfate attack was an outside-in process, the sulfate attack products firstly formed on the surface, which was more obvious to increase the flexural strength at the sulfate attack early

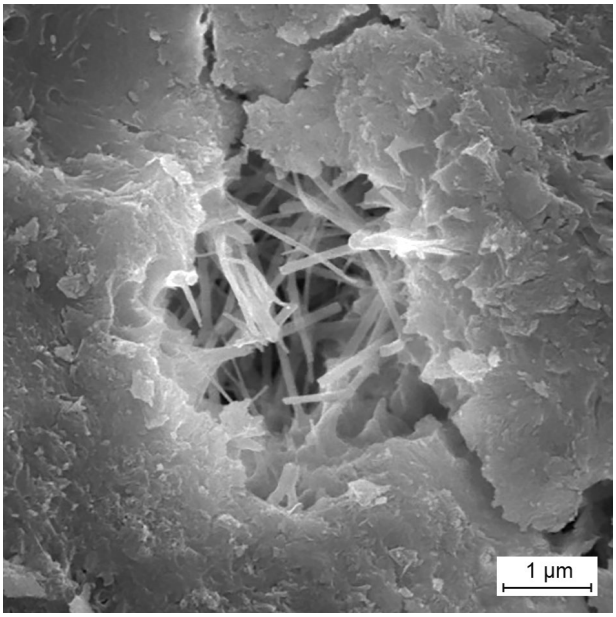

a)

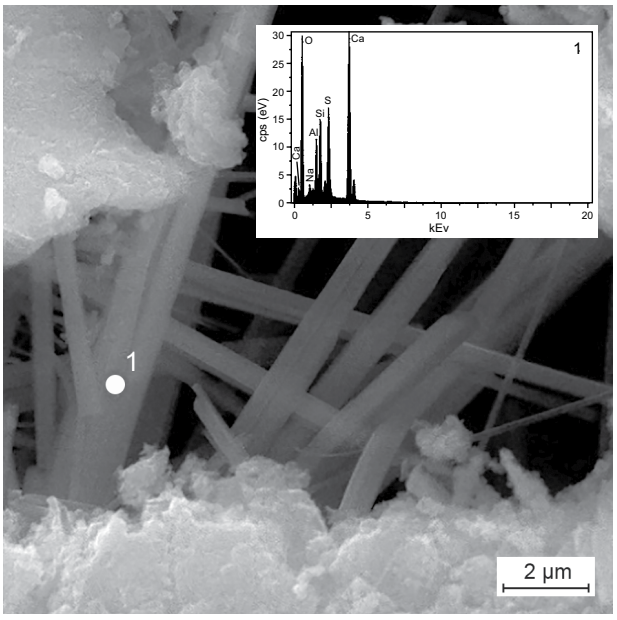

b)

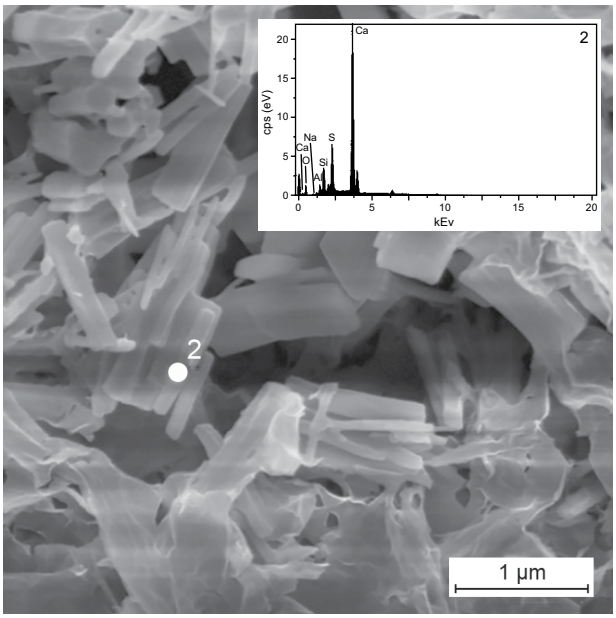

c)

Figure 7. SEM images and EDS of the cement paste samples cured in a 10 wt. % Na_2SO_4 solution up to 360 days.

age. The samples with the FA and CG showed a higher strength than the C samples, more of the sulfate solution migrated inside which contributed to this condition. With a cured time up to 180 days, a higher strength ration of the C samples is shown as more sulfate attack products were formed. A higher compact structure was formed and a strength enhancement occurred. Figure 7a showed the ettringite fill in the pores, which might prove part of the strength before destroying the pores.

When the mortar samples are cured in the 10 wt. % Na_2SO_4 solution up to 360 days, a strength decrease was observed and it indicated that damage caused by the sulfate attack occurred. A comparable strength ratio with the C Ref samples was observed, which was related to the lesser attack products (showed in Figure 6). The FA-added samples showed a lower strength ratio than the C Ref samples and higher strength ratios than the C samples, which might be explained by two reasons: (1) the FA that replaced part of the cement decreased the formation of the sulfate attack products, thus a higher strength resulted that in than C samples; (2) the weak binding of the unhydrated FA particles and hydration products might be easily cracked under sulfate attack [32], thus a lower strength resulted than that in the C Ref samples.

The flexural and compressive strength of the mortar samples cured in the 10 wt. % Na_2SO_4 solution at 360 days is shown in Figure 8. The control samples showed the highest strength loss after the sulfate attack at 360 days, a 20 % strength loss was shown. For the samples with the CG addition, the strength loss was reduced with an increase in the CG-added dosage and the CG30 samples showed a strength enhancement. The decrease in the strength loss was due to the high-level cement replacement that retarded the sulfate and reduced the sulfate attack product content (as shown in Figure 9). In addition, the depleted structure might create a large space for the sulfate attack products and the deterioration time becomes delayed. For the FA-added samples, a lower strength loss was exhibited than that in the C samples and the reason was the same with the CG-added samples. However, the strength loss of the FA10 samples was higher than the CG10 samples, and also the FA20, FA30 samples compared with the CG20, CG30 samples, respectively. This indicated that the CG could improve the sulfate attack resistivity of the cement mortar and this effect was better when compared with the FA. It might be attributed to the high pozzolanic reactivity of the CG while the CH content reacting with sulfate solution was reduced.

For the compressive strength change, the C samples showed the highest strength loss of 12.4 %, which was lower than the flexural strength loss, which was due to the attack that firstly occurred on the surface and it was more obvious in the flexural strength change. The CG10/CG20 samples showed a 5.6/3.2 % strength loss, respectively. The CG30 samples showed a strength increase of about 1.4 %. Meanwhile, the FA10 and FA20 samples showed higher strength increases. The low reactivity of the FA caused the large porosity and more sulfate attack products (as shown in Figure 9) filled the pores. The large porosity provided more space for the sulfate attack products and damage did not occur. These effects resulted in the strength increase. The FA30 samples showed a compressive strength loss of 1.6 % as the reason is that more sulfate solution entered inside and reacted with the hydration products, and then damage was observed.

Length change of cement mortar after sulfate attack

The formation of sulfate attack products, such as ettringite and gypsum, increased the solid volume and expansion resulted. The length changes of the cement mortar after the sulfate attack are shown in Figure 9. The control samples showed the highest length change of about 0.035 % at 360 days when cured in the sulfate solution. This was consistent with the largest strength loss in Figure 8, as more sulfate attack products caused

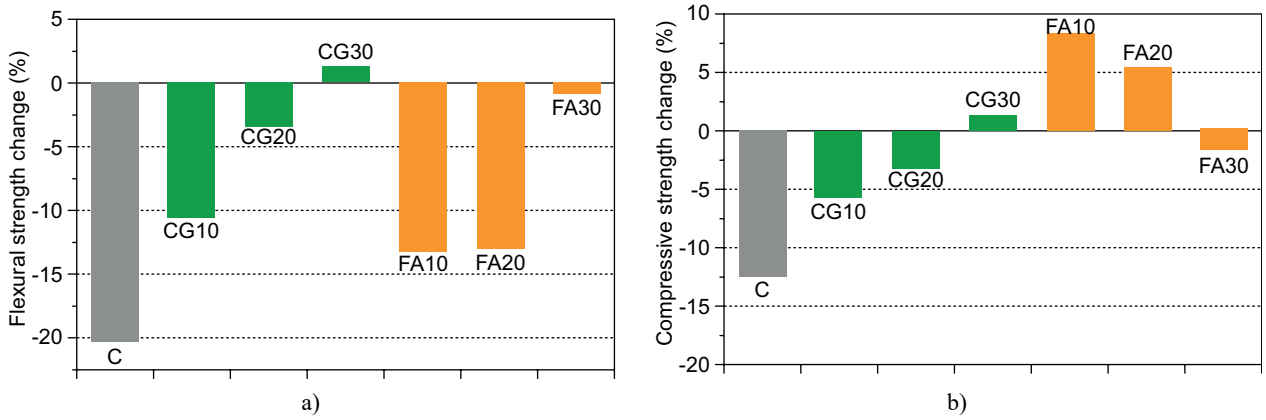

Figure 8. Flexural (a) and compressive strength of the mortar samples cured in a 10 wt. % Na_2SO_4 solution at 360 days (the negative values represent the strength loss and the positive values represent the strength increase when compared to the samples cured in the CH solution).

these results. When the sulfate attack time is up to 180 days, the FA10 and FA30 samples showed a slightly higher length change when compared with the CG-added samples. A similar length change was revealed by the CG and FA added samples when the curing time in the 10 wt. % Na_2SO_4 solution is up to 360 days, and the minimum value of 0.024 % was shown by the CG30 samples. Considering these results, it can be concluded that the FA and CG both reduced the expansion under the sulfate attack and a better performance was observed with the CG. These results were consistent with the strength development and loss in Section 3.2.

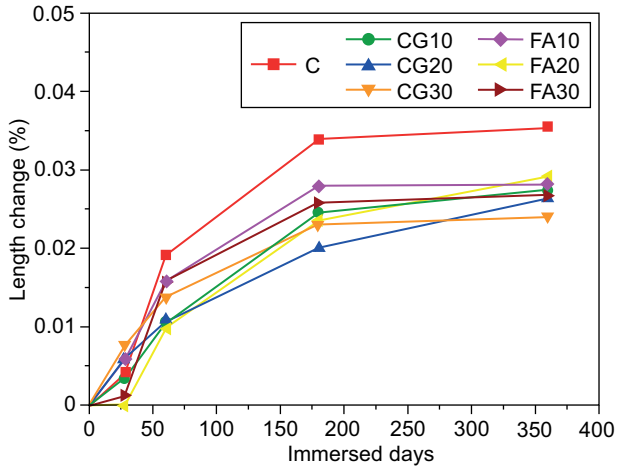

Figure 9. The length change of the cement mortar cured in a 10 wt. % Na_2SO_4 solution up to 360 days.

Strength of cement concrete after sulfate attack

The compressive strength development of the cement concrete cured in the 10 wt. % Na_2SO_4 solution after 90 and 120 wet-dry cycles is shown in Figure 10. A strength increase was observed with all the samples at 90 wet-dry cycles. The sulfate attack products were not enough to damage the concrete structure, but served to fill the voids/pores. A strength increase was observed, which was consistent with the mortar strength change of the mortars before 180 days in Figure 5. The CG20/CG30 and FA20/FA30 samples showed a higher strength change, which might be due to the loose structure leading to more of the sulfate solution entering inside the concrete, as well as the sulfate attack products and recrystallisation sulfate filling the pores [32]. Finally, a denser structure formed which revealed a strength increase. When the wet-dry cycles increased to 120, the control samples revealed the highest strength loss, which was same as the mortar in Figure 8. The CG10 and CG20 samples showed a strength loss while an increased strength was shown by the CG30 samples. The high replacement level of the cement by the CG alongside with the pozzolanic reactivity consumed more CH and reduced the sulfate attack products (as shown in Figure 6), and the damage was delayed or avoided. The FA10 and FA20 samples also showed a strength loss and the FA30 sample showed a strength increase, the reason was the same as the CG-added samples.

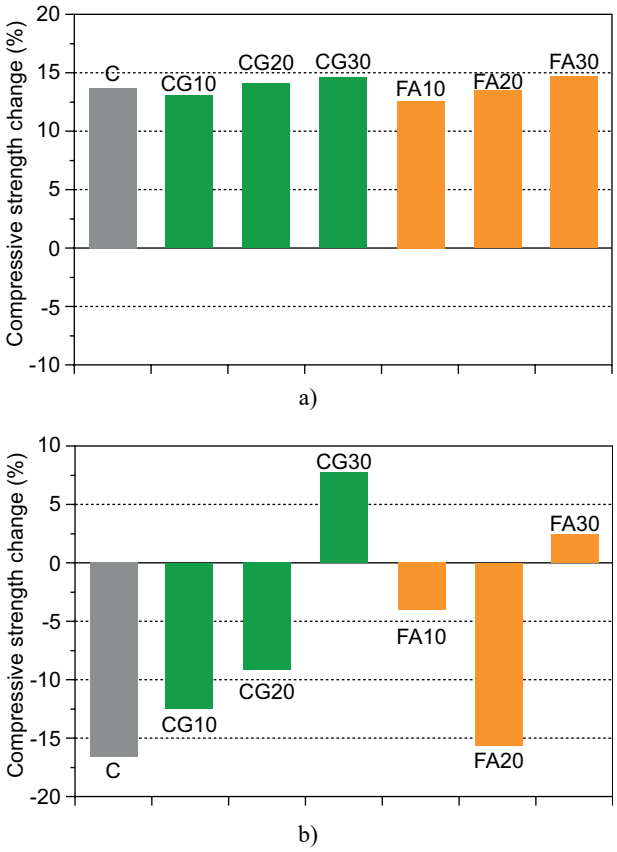

Figure 10. Compressive strength of the concrete samples cured in a 10 wt. % Na_2SO_4 solution (a) 90 (b) 120 wet-dry cycles (the negative values represent the strength loss and the positive values represent the strength increase when compared with the samples cured in the CH solution).

CONCLUSION

In this paper, the effects of coal gangue on the sulfate attack resistivity of cement-based materials in terms of its mechanical properties, volume stability and sulfate attack products were studied. The effects were also compared with fly ash added samples. The following conclusions can be drawn:

- Calcined coal gangue has a higher pozzolanic reactivity than class F fly ash.
- The addition of calcined coal gangue significantly improved the sulfate attack resistivity of the cement-based materials, specifically, it results in a reduction in the strength loss of the cement mortar and concrete, and expansion of the cement mortar under the sulfate

attack. The coal gangue also improved the sulfate attack resistivity of the cement-based materials under the wet-dry cycles of the sulfate attack.

- When compared with the fly ash added samples, the coal gangue ones exhibited better improvement in the sulfate attack resistivity through the analysis of the strength loss and expansion results.
- The higher sulfate attack resistivity of the coal gangue-added samples was attributed to the replaced part of the cement and reduced sulfate attack products, and the pozzolanic reactivity consumed part of the CH.

REFERENCES

1. Aziz M. A. E., Aleem S. A. E., Heikal M., Didamony H. E. (2005): Hydration and durability of sulphate-resisting and slag cement blends in Caron's Lake water. *Cement and Concrete Research*, *35*(8), 1592-1600. doi: 10.1016/j.cemconres.2004.06.038
2. Liu Z., Zhang F., Deng D., Xie Y., Long G., Tang X. (2017): Physical sulfate attack on concrete lining – A field case analysis. *Case Studies in Construction Materials*, *6*, 206-212. doi:10.1016/j.cscm.2017.04.002
3. Schmidt T., Lothenbach B., Romer M., Neuenschwander J., Scrivener, K. (2009): Physical and microstructural aspects of sulfate attack on ordinary and limestone blended Portland cements. *Cement and Concrete Research*, *39*(12), 1111-1121. doi: 10.1016/j.cemconres.2009.08.005
4. Santhanam M., Cohen M. D., Olek J. (2002): Mechanism of sulfate attack: A fresh look: Part 1: Summary of experimental results. *Cement and Concrete Research*, *32*(6), 915-921. doi: 10.1016/S0008-8846(02)00724-X
5. Rozière E., Loukili A., El Hachem R., Grondin F. (2009): Durability of concrete exposed to leaching and external sulphate attacks. *Cement and Concrete Research*, *39*(12), 1188-1198. doi: 10.1016/j.cemconres.2009.07.021
6. Monteiro P. J., Kurtis K. E. (2003): Time to failure for concrete exposed to severe sulfate attack. *Cement and Concrete Research*, *33*(7), 987-993. doi: 10.1016/S0008-8846(02)01097-9
7. Wang Q., Wang D., Chen, H. (2017): The role of fly ash microsphere in the microstructure and macroscopic properties of high-strength concrete. *Cement and Concrete Composites*, *83*, 125-137. doi: 10.1016/j.cemconcomp.2017.07.021
8. Sezer G.I. (2012): Compressive strength and sulfate resistance of limestone and/or silica fume mortars. *Construction and Building Materials, 26*, 613–618. doi: 10.1016/j.conbuildmat.2011.06.064
9. Mostofinejad D., Nosouhian F., Nazari-Monfared H. (2016): Influence of magnesium sulphate concentration on durability of concrete containing micro-silica, slag and limestone powder using durability index. *Construction and Building Materials,* 117, 107–120. doi: 10.1016/j.conbuildmat. 2016.04.091
10. Hossack A.M., Thomas M.D.A. (2015): The effect of temperature on the rate of sulfate attack of Portland cement blended mortars in Na_2SO_4 solution. *Cement and Concrete Research*, *73*, 136-142. doi: 10.1016/j.cemconres.2015.02.024
11. Chen F., Gao J.M., Qi B., Shen D.M. (2017): Deterioration mechanism of plain and blended cement mortars partially exposed to sulfate attack. *Construction and Building Materials,* 154, 849-856. doi: 10.1016/j.conbuildmat.2017.08.017
12. Kunther W., Lothenbach B., Skibsted J. (2015): Influence of the Ca/Si ratio of the C–S–H phase on the interaction with sulfate ions and its impact on the ettringite crystallization pressure. *Cement and Concrete Research*, *69*, 37-49. doi: 10.1016/j.cemconres.2014.12.002
13. Panesar D. K., Zhang R. (2020): Performance comparison of cement replacing materials in concrete: Limestone fillers and supplementary cementing materials – A review. *Construction and Building Materials*, *251*, 118866. doi: 10.1016/j.conbuildmat.2020.118866
14. Chen Y., Zhou S., Zhang W. (2008): Effect of coal gangue with different kaolin contents on compressive strength and pore size of blended cement paste. *Journal of Wuhan University of Technology-Mater. Sci. Ed.*, *23*(1), 12-15.
15. Cao Z., Cao Y., Dong H., Zhang J., Sun C. (2016): Effect of calcination condition on the microstructure and pozzolanic activity of calcined coal gangue. *International Journal of Mineral Processing*, *146*, 23-28. doi: 10.1016/j.minpro.2015.11.008
16. Ilić B. R., Mitrović A. A., Miličić L. R. (2010): Thermal treatment of kaolin clay to obtain metakaolin. *Hemijska industrija*, *64*(4), 351-356. doi: 10.2298/hemind100322014i
17. Hu X., Zhao, Z. Wang C., Zhang (2013): Research progress on activation of kaolin minerals by microwave irradiation. *Multipurp. Util. Miner. Resour., 2*, 20–23 (in Chinese).
18. Xu X., Lao X., Wu J., Zhang Y., Xu X., Li K. (2015): Microstructural evolution, phase transformation, and variations in physical properties of coal series kaolin powder compact during firing. *Applied Clay Science*, *115*, 76-86. doi: 10.1016/j.clay.2015.07.031
19. Song X., Gong C., Li D. (2004): Study on structural characteristic and mechanical property of coal gangue in activation process. *Journal-Chinese Ceramic Society*, *32*(3), 358-363.
20. Huang G., Ji Y., Li J., Hou Z., Dong Z. (2018): Improving strength of calcinated coal gangue geopolymer mortars via increasing calcium content. *Construction and Building Materials*, *166*, 760-768. doi: 10.1016/j.conbuildmat.2018.02.005
21. Li D., Song X., Gong C., Pan Z. (2006): Research on cementitious behavior and mechanism of pozzolanic cement with coal gangue. *Cement and Concrete Research*, *36*(9), 1752-1759. doi: 10.1016/j.cemconres.2004.11.004
22. Zhang Y., Ling T. C. (2020): Reactivity activation of waste coal gangue and its impact on the properties of cement-based materials–A review. *Construction and Building Materials*, *234*, 117424. doi: 10.1016/j.conbuildmat.2019.117424
23. Yang J., Su Y., He X., Tan H., Jiang Y., Zeng L., Strnadel B. (2018): Pore structure evaluation of cementing composites blended with coal by-products: Calcined coal gangue and coal fly ash. *Fuel Processing Technology*, *181*, 75-90. doi: 10.1016/j.fuproc.2018.09.013
24. Yi C., Ma H., Zhu H., Li W., Xin M., Liu Y., Guo Y. (2018): Study on chloride binding capability of coal gangue based cementitious materials. *Construction and Building Materials*, *167*, 649-656. doi: 10.1016/j.conbuildmat.2018.02.071

25. Guo W., Zhu J., Li D., Chen J., Yang N. (2010): Early hydration of composite cement with thermal activated coal gangue. *Journal of Wuhan University of Technology-Mater. Sci. Ed.*, *25*(1), 162-166.
26. GB/T 17671-1999 (2019). Method of testing cements-determination of strength.
27. GB/T 596-2017 (2017). Fly ash used for cement and concrete.
28. ASTM C 1012/C1012M (2015). *Standart Test Method for Length Change of Hydraulic Cement Mortars Exposed to Sulfate Solution* Vol. 04.01, Annual Book of ASTM Standards, West Conshohocken, PA.
29. Wee T. H., Suryavanshi A. K., Wong S. F., Rahman A. A. (2000): Sulfate resistance of concrete containing mineral admixtures. *Materials Journal*, *97*(5), 536-549. doi: 10.1016/S0886-7798(01)00020-7
30. Guo Z., Wang Y., Hou P., Shao Y., Zuo X., Li Q., et al. (2019): Comparison study on the sulfate attack resistivity of cement-based materials modified with nanoSiO_2 and conventional SCMs: Mechanical strength and volume stability. *Construction and Building Materials*, *211*, 556-570. doi: 10.1016/j.conbuildmat.2019.03.235
31. Demir I., Güzelkücük S., Sevim Ö. (2018): Effects of sulfate on cement mortar with hybrid pozzolan substitution. *Engineering Science and Technology, an International Journal*, *21*(3), 275-283. doi: 10.1016/j.jestch.2018.04.009
32. Qi B., Gao J., Chen F., Shen D. (2017): Evaluation of the damage process of recycled aggregate concrete under sulfate attack and wetting-drying cycles. *Construction and Building Materials*, *138*, 254-262. doi: 10.1016/j.conbuildmat.2017.02.022